IEEE Access
Multidisciplinary ⋮ Rapid Review ⋮ Open Access Journal

Received March 15, 2021, accepted April 28, 2021. Date of publication xxxx 00, 0000, date of current version xxxx 00, 0000.

Digital Object Identifier 10.1109/ACCESS.2021.3085859

A Valid Model for Prediction Tibiofemoral Force for Healthy People Based on Static Optimization

ALI MAMDOUH MOHAMED[1,2] **AND RONGLEI SUN**[1]

[1]State Key Laboratory of Digital Manufacturing Equipment and Technology, School of Mechanical Science and Engineering, Huazhong University of Science and Technology, Wuhan 430074, China
[2]Mechanical Power Engineering Department, Faculty of Engineering, Tanta University, Gharbeya 31511, Egypt

Corresponding author: Ronglei Sun (ronglei@hust.edu.cn)

This work was supported in part by the National Natural Science Foundation of China under Grant U1613206, and in part by the China Scholarship Council.

ABSTRACT The musculoskeletal model plays an important role in the investigation of human lower limb diseases. Although different methods are used for musculoskeletal models, the prediction of the tibiofemoral and muscle forces still needs more improvements. This paper introduces a model for the lower limb; 3-DOF hip, 1-DOF knee, and 3-DOF ankle. The model estimates the tibiofemoral and muscle forces based on static optimization. The shank and the foot are considered as one element to avoid the high-cost computation of the traditional inverse dynamic method. The direction of the tibiofemoral force is estimated based on the analytical method to tune the weight factors of the predicted force. Two subjects (A and B) performed walking at 1m/s for about 5 gait cycles with recording the kinematics, ground reaction force (GRF), and foot center of pressure (CoP) and electromyographic (EMG) signals. A static optimization technique was performed to predict the tibiofemoral and 6 lower limb muscles forces based on the 2nd-Newton law in three-dimensional (3D). Muscles moment arms were verified by compared to measured data in the literature. The validity of the model was guaranteed by testing the model on a subject of total knee replacement (TKR) and compared the predicted tibiofemoral force with the measured one. The predicted tibiofemoral forces had the root mean square error (RMSE) of 0.19, 0.56, and 0.43 BW for TKR subject, subject A and subject B, respectively. The predicted muscles force was validated by comparing it to EMG signals. The analysis and the validation of the model showed that it could be used for different activities like walking and running and assessment rehabilitation devices such as knee brace.

INDEX TERMS Musculoskeletal model of the lower limb, tibiofemoral force prediction, muscle force estimation, static optimization.

I. INTRODUCTION

The knee plays an important role in the balance of the whole body. The knee shows different characteristics such as various load support, according to the activities [1], and different kinematics according to gender [2], and healthy conditions (i.e. healthy vs. osteoarthritis)[3]. The knee diseases such as osteoarthritis and anterior circulate ligament (ACL) deficiency encourage scientist to develop a musculoskeletal model to describe the cause and prognosis of these diseases; like cartilage deformation[4], [5]. Also, to introduce different treatment and rehabilitation strategies according to the symptoms and from the engineering point of view according to the kinematic and dynamics of the lower limb [6]. The diversity of the human body structure like the bone geometries appearing in the kinematics and knee points of contact [2], [7], the muscles, and the ligaments parameters [8], [9], overcomes having a generic musculoskeletal model. Different knee features overcome deciding the suitable treatment for diseases

The subject-specific model showed reasonable results for the analysis of knee motion and predicting the tibiofemoral force [10]. While the prediction of the tibiofemoral force has great attention by researchers [11], different models were introduced using numerical knee model [12], the surrogate knee model based on an artificial neural network[13], and the whole lower limb model [14]. Moreover, ASME held many competitions to introduce a model that can predict this force [6], [15] using different subjects with TKR with implant e-tibia. The major difficulty in the prediction process is an indeterminate system of equations representing the knee

The associate editor coordinating the review of this manuscript and approving it for publication was Wen-Sheng Zhao.

motion due to the muscles redundancy. Researchers and organizations exerted great effort to predict tibiofemoral force.

Unfortunately, the muscles can't be measured directly outside the surgery room except for small invasive measurements in superficial tendons like the Achilles [16]. The muscle redundancy and the indeterminate system of equations could be solved using optimization for the muscles-tendon force. The cost function for the optimization process was based on the sum square of the muscle force, stress, and activation [17], with the known muscle moment arm. Buford [18] and Spoor [19] used cadaver lower limb and they measured the excursion of the muscles to represent the moment arm. The moment arm could be analytically estimated using two methods the tendon excursion and the cross product [20]. Arnold [8], introduced a musculoskeletal model based on the muscles tendon excursion to estimate the moment arm while anybody software is based on the cross-product method.

There were two approaches for muscles force prediction; the forward and inverse dynamic approach [21]. Using the forward dynamic approach; the activations of the muscles or joints torques are known, and integration of the system equations is performed to find the kinematics of the lower limb and compared with the measured one [22], [23]. The inaccurate measurements of the muscle activation and the muscle torque hindered the prediction of the muscle force using this approach. The inverse dynamic approach is preferred by many researchers due to its simplicity. The forces and moments at each segment peripherals are found then these forces and moments are transferred to the next segment. However, this method suffered from dealing with complexity and many unknowns. This problem was solved using the wrench approach [24], [25] but it is not conventional like 2nd Newton law for describing the motion for biomechanical systems.

The goal of this study is two folds. Firstly, to introduce a simple method for predicting the muscles and tibiofemoral forces using the 2nd Newton law with an analytical method for predicting the force in 3D. The model presents the shake and the foot as one element to reduce the complexity and the unknown forces. Secondly, to validate the model for two healthy subjects by comparing the predicted tibiofemoral forces to the in vivo data [6] of a TKR subject and the data in the literature. Additionally, the model is implemented on the TKR subject as ground truth for the model validation.

II. METHOD

A. EXPERIMENTAL DATA

The experimental data are based on open source data HUMOD [26] for a healthy female subject (27 years, 1.61 m, 57 kg) and a male subject (32 years, 1.79 m, 85 kg) performed tials for about 100 sec within walking speed 1m/s. The whole body had 35 reflective markers, the kinematics of the lower limb could be calculated after recording markers positions at 500 Hz with a three-dimensional motion capture system consisting of four Oqus 310+ cameras and six Oqus 300+ cameras (Qualisys, Sweden) Fig.1. The EMG signals of fourteen

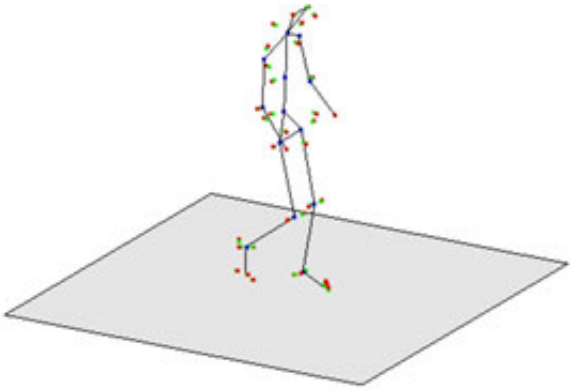

FIGURE 1. The subject walks at 1m/sec and the markers are used to record the kinematics, [26].

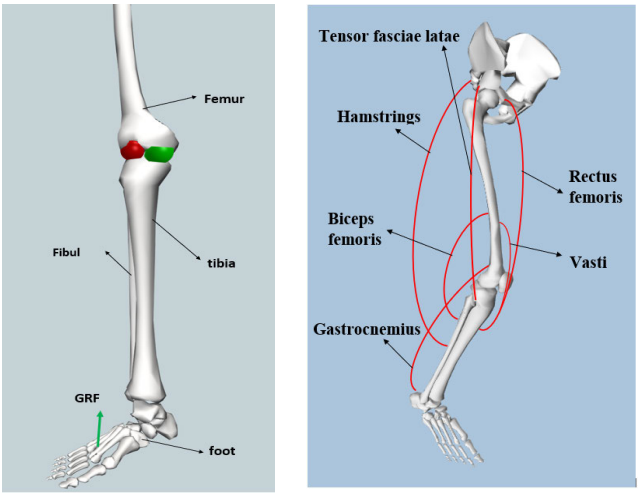

FIGURE 2. The musculoskeletal model and muscles affecting the knee motion.

selected muscles in both legs were recorded at 2000 Hz and filtered to bandwidth between 20 Hz and 450 Hz. GRFs were measured using two force places with four multi-axis force sensors (Kistler, Switzerland) to measure the medial and the lateral GRF. The GRF data were recorded at 1000 Hz.

B. THE LOWER LIMB

The model of the lower limb was based on representing the hip as 3-DOF, the knee as 1-DOF, and the ankle as 3-DOF as shown in Fig.2. The method used here was to reduce the complexity of the system equations by decreasing the number of unknown forces [27], [28] unlike the traditional inverse dynamic method. While other models transfer the force from one joint to the next, herein the shank and the foot were represented as one element and the moment of inertia was calculated for each segment w.r.t femur origin using the parallel axes theorem.

The equation of motion representing the external force (i.e. GRF), the muscle and tibiofemoral force were represented by (1) and (2), as shown at the bottom of the next page, using 2nd Newton law in 3D, where m is the mass of two segments,

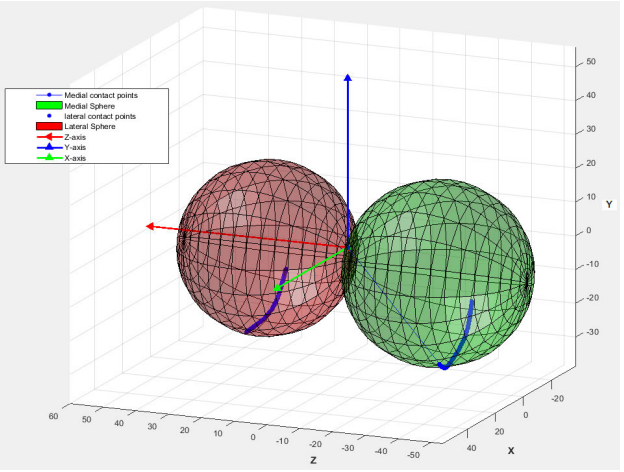

FIGURE 3. The medial and lateral femur condyles as a part of two spheres and the tibiofemoral contact points.

GRF_j, $F_{cont\,j}$, $F_{mus\,j}$, and W_j are the GRF, muscles' forces and the weight in X-Y-Z axes, respectively, and j stands for X-Y-Z axes and n represents the muscles used. Additionally, $\ddot{x}$, $\ddot{y}$, *and*$\ddot{z}$ are the linear acceleration components of the shank and the foot the center of mass (CoM) in 3D. The vectors r_{GRM}, r_{cont}, r_{musc}, and r_g are moment arm for GRF at CoP position, muscle force at the insertion points (via points), tibiofemoral force at the contact points between the femur and the tibia, and the weight of each segment at CoM w.r.t the femur origin. Also, I_{xx}, I_{yy}, I_{zz} are the 2nd moment of inertia for each segment [26]. The angular velocity and acceleration around the Cartesian coordinates are $\dot{\theta}_x, \dot{\theta}_y, \dot{\theta}_z, \ddot{\theta}_x, \ddot{\theta}_y, \ddot{\theta}_z$

$$\begin{bmatrix} GRF_x \\ GRF_y \\ GRF_z \end{bmatrix} + \begin{bmatrix} F_{cont-x} \\ F_{cont-y} \\ F_{cont-z} \end{bmatrix} + \sum_{i=1}^{i=n} \begin{bmatrix} F_{\mathrm{i}\,musc\,x} \\ F_{i\,musc\,y} \\ F_{\mathrm{i}\,musc\,z} \end{bmatrix} + \begin{bmatrix} w_x \\ w_y \\ w_z \end{bmatrix} = m \begin{bmatrix} \ddot{x} \\ \ddot{y} \\ \ddot{z} \end{bmatrix} \quad (1)$$

C. KNEE MODEL

The medial and lateral femoral condyles are represented as part of spheres as shown in Fig.3 with the surface represented by (3) and (4). The frame directions are based on the international society of biomechanics recommendations (ISB) [29]. The anterior-posterior represents the positive X-axis; the medial-lateral represents the positive Z-axis and the superior-inferior represents the positive Y-axis Fig. 3. The origin of the femur is considered as the midpoint between the center of the two femur condyles where a, b, and c are the center of the two femur condyles and r_{fm} and t_{fl} are the radii for the medial and lateral femur condyles, respectively.

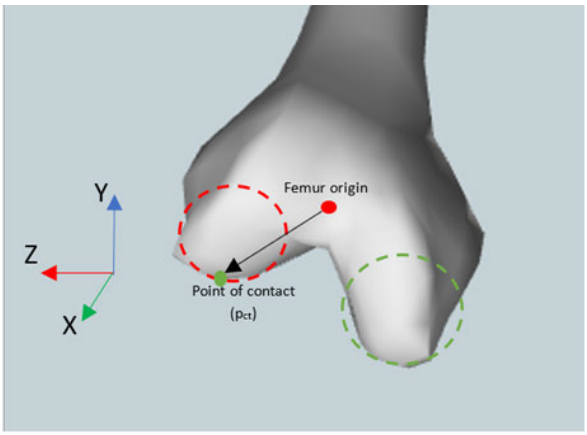

FIGURE 4. The contact point (P_{ct}) w.r.t the femur origin.

For the medial femur condyle

$$(x-a_1)^2+(y-b_1)^2+(z-c_1)^2=r_{fm}^2 \quad (3)$$

For the lateral femur condyle

$$(x-a_2)^2+(y-b_2)^2+(z-c_2)^2=r_{fl}^2 \quad (4)$$

The points of contact between the femur and the tibia were represented by a fixed distance in the medial and lateral direction about 20 mm from the anterior-posterior axis, and as a function of the flexion angle along the anterior-posterior axis direction, based on the regression method [30] as shown in Fig 3. A fixed distance of about 25 mm in the inferior direction was considered for the simulation of the points of contact in 3D. The direction of the force on the medial and lateral femur condyles is based on points of contact between the femur and the tibia as illustrated in Fig.4. The vector at each femur condyle is differentiated w.r.t X-axis and Z-axis and using the cross product to get normal vector at the points of contact [31] as expressed by (5) and illustrated in Fig.5.The details derivation can be found in Appendix A

$$\hat{n}_f = \frac{n_f}{\| n_f \|} = \frac{\left.\frac{\partial y}{\partial x}\right|_{(x_c,z_c)} \hat{i} - \hat{j} + \left.\frac{\partial y}{\partial z}\right|_{(x_c,z_c)} \hat{k}}{\sqrt{\frac{r_{fm}^2}{r_{fm}^2-(x-a_1)^2-(z-c_1)^2}}} \quad (5)$$

D. MUSCLES MODEL

The muscles were represented by 6 muscles that passed through the knee, hip and ankle [32]; the rectus femoris, tensor fasciae latae, hamstring, biceps femoris, vasti, and gastrocnemius Fig.2. The origin, via points, the insertion points and physiological cross-section area (PCSA) of the muscles were based on the data of Klein Horsman 2007 [9]. The moment arm of the muscles was based on a straight line

$$r_{GRM} \times GRF + r_g \times w + r_{cont} \times F_{cont} + r_{\mathrm{i\,musc}} \times F_{i\,musc} = \begin{bmatrix} I_{xx}\ddot{\theta}_x \\ I_{yy}\ddot{\theta}_y \\ I_{zz}\ddot{\theta}_z \end{bmatrix} + \begin{bmatrix} (I_{zz}-I_{yy}) \\ (I_{xx}-I_{zz}) \\ (I_{yy}-I_{xx}) \end{bmatrix} \begin{bmatrix} \dot{\theta}_y\dot{\theta}_z \\ \dot{\theta}_x\dot{\theta}_z \\ \dot{\theta}_x\dot{\theta}_y \end{bmatrix} \quad (2)$$

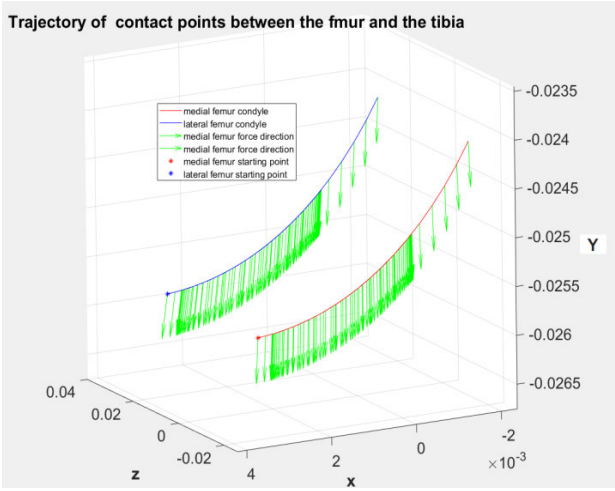

FIGURE 5. The direction of the tibiofemoral force during the stance phase.

between the origin and the insertion, and for hamstring using via points. The vasti and the rectus femoris were based on the motion of the patella w.r.t the femur using the helical axis [9]. The moment arm was compared to measured data from literature; Arnold [8], Buford [18] and Spoor as shown in Fig.6.

III. OPTIMIZATION TECHNIQUE

Static optimization are used for the estimation of the muscles and tibiofemoral forces by performing minimization of the cost function defined in (6), where F represents the muscle and tibiofemoral forces, ω is a weight vector. Additionally, A_{equ} is a matrix of the cross product between the moment arm and unity vector for each force line of action in 3D, B_{equ} is a vector of the moment affecting the knee in 3D, and C is the vector of the total force constraining the motion of the knee, details are in APPENDIX B.

$$\min_{F} \mathrm{J} = \sum F^T \omega F \tag{6}$$

$$subject\ \text{to} \begin{cases} A_{equ}F = B_{equ} \\ lb \leq F_{musc} \leq ub \\ \sum F_{musc} + F_{cont} = C \end{cases} \tag{7}$$

The weight and constraints for the criteria (i.e. cost function) played an important role in the force prediction. The weight of muscles is considered as 1/PSCA^2. The lower boundary for all forces was negative infinity. However, the upper boundary (ub) was the maximum isometric muscle force, 61 N/cm^2 times the PSCA [8], whereas for the tibiofemoral force it was infinity. The linear and nonlinear equality constraints were based on the 2nd Newton law for linear and rotational motion w.r.t the femur origin in (1B, 2B) APPENDIX B. The forces that affect the tibia by the patella tendon were considered equal to the force of the vasti and rectus femoris but in the opposite direction.

TABLE 1. The medial and the lateral tibiofemoral force prediction (BW) comparing to the literature data.

	Medial tibia		Lateral tibia	
Authors	1st Peak	2nd Peak	1st Peak	2nd Peak
Moissenet 2016;[37]	1.38	0.7	0.46	0.55
Meireles 2017; [38]	2.2	1.8	1.2	1.2
VanRossom 2018;[39]	1.8	1.9	1.3	1.0
Dumas 2020;[7]	1.6	1.9	1.0	0.6
Subject (A)	2.34±0.1	1.37±0.2	1.65±0.2	0.89±0.4
Subject (B)	1.6±0.2	0.5 ±0.4	1.48±0.3	0.6±0.1

TABLE 2. RMSE and (R^2) for the medial, lateral and total TIBIOFEMORAL force (TF) in BW.

Tibia Compartment	Subject A	Subject B	subject TKR
Medial TF (R^2)	0.3(0.54)	0.15(0.8)	0.14 (0.86)
Lateral TF (R^2)	0.16(0.41)	0.12(0.3)	0.09(0.75)
Total TF (R^2)	0.56(0.05)	0.43(0.2)	0.19(0.84)

TABLE 3. RMSE and (R^2) for the predicted muscles forces in BW.

Muscles	Subject A	Subject B
Gastrocnemius	0.18 (0.32)	0.28(0.55)
Rectus femoris	0.04 (0.83)	0.02(0.64)
Vasti	0.10 (0.53)	0.09(0.26)
biceps	0.04 (0.29)	0.06(0.67)

IV. RESULTS

The force of the medial, lateral, and total tibiofemoral compartments are presented in Fig.7 for subjects A and B where the tibiofemoral forces were compared to in vivo data of TKR subject [6], [33] from the 4th grand challenge competition. Moreover, the predicted tibiofemoral forces were compared to other models in the literature, for the 1st and 2nd peak values of the medial and lateral tibiofemoral force as shown in Table 1. Additionally, the analysis of tibiofemoral forces using RMSE and co-efficient of determination (R^2) was presented in Table 2. The predicted muscles force patterns were compared to the corresponding EMG signals after scaling, Fig. 8. The agreement between the predicted muscles' force and the EMG signals was verified by the co-efficient of concordance [34] where it was 0.66 and 0.96 for subject A and B, respectively. The RMSE and (R^2) for the predicted muscles were shown in Table 3.

V. VALIDATION FOR TIBIOFEMORAL FORCE PERDITION USING TKR SUBJECT

A subject of TKR with e-tibia from the 4thh grand challenge competition [6] performed walking at low speed was used

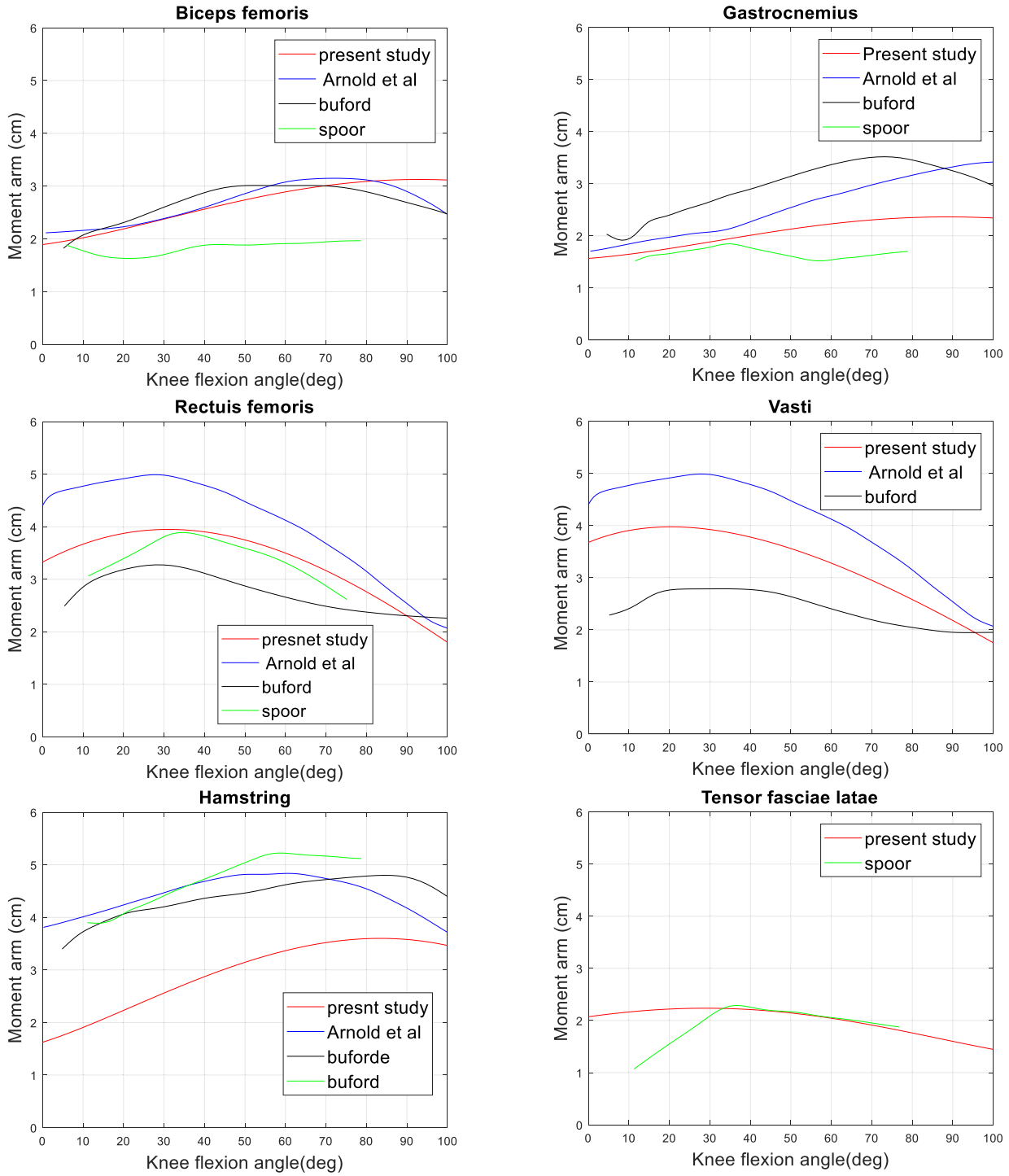

FIGURE 6. **Muscles moment arm. the present study (red line), the model by Arnold *et al.* [8] (blue line) the measured by Buford [18] (black line) and Spoor [19] (green line).**

to validate the tibiofemoral force perdition. The OpenSim model [35] was used to estimate the joint angles using inverse kinematics. The SCORE method [36] was used to find the hip and the knee joint positions during the stance phase. The prediction force was compared to the in vivo data measured from e-tibia, Fig. 9. The medial tibiofemoral force had RMSE 0.14 BW (R2 = 0.86) where the 1st and the 2nd peak have values of 1.35 ± 0.2 BW and 1.3 ± 0.09 BW, respectively. The lateral tibiofemoral force had RMSE 0.09 BW (R^2 = 0.75) where the 1st and the 2nd peak have values of 0.13 ± 0.03 BW and 0.89 ± 0.09 BW, respectively. Additionally, the total tibiofemoral force prediction had better results where

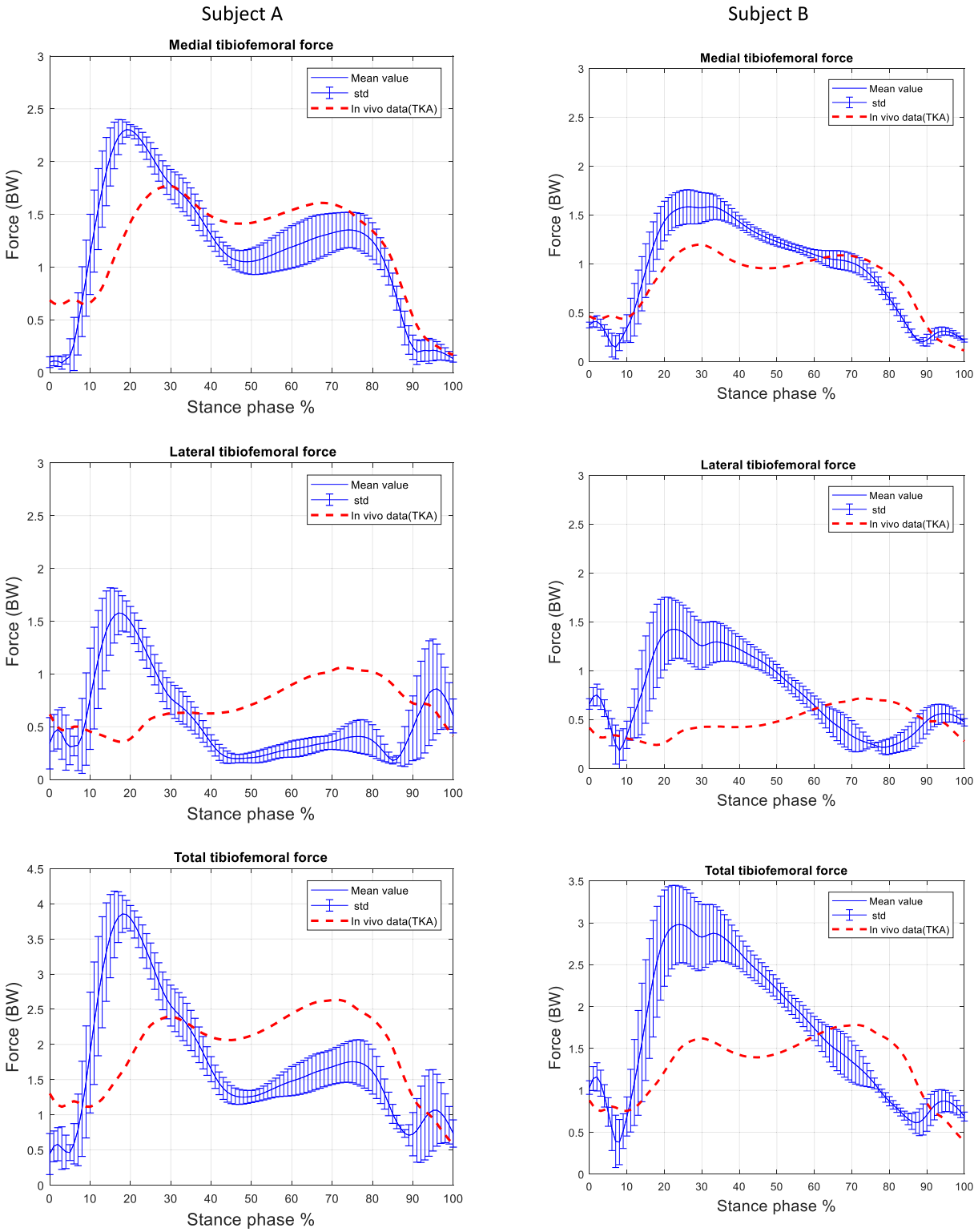

FIGURE 7. The tibiofemoral force prediction for subjects A and B. the mean value for the prediction force(solid blue line), standard deviation,(std in vertical bars), and the in vivo data[6] (in dotted red).

RMSE was 0.19 BW ($R^2 = 0.84$) and the forces at the 1st and 2nd peaks were 1.47 ± 0.25 and 2.3 ± 0.17 BW, respectively.

VI. DISCUSSION

A musculoskeletal model of the lower limb was developed to estimate the tibiofemoral force and the muscles force

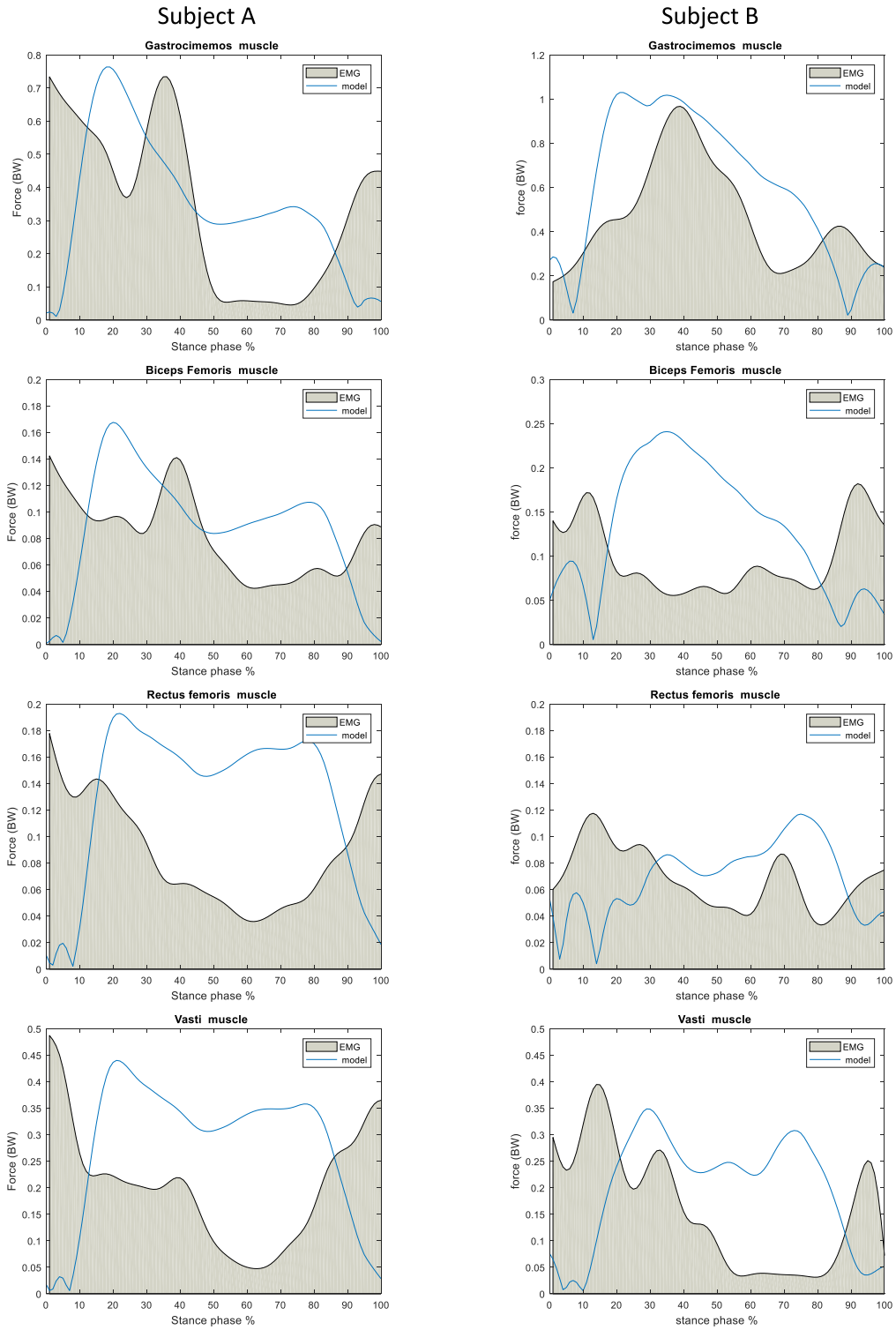

FIGURE 8. The predicted muscles force (blue line) is compared to the corresponding EMG signals (shaded area).

based on static optimization. The model used two subjects A and B performed walking at 1m/sec for about 5 gait cycles, recording the kinematics, GRFs and CoPs, and the EMG signals. All data were processed and filtered to delete the noise in the signals then used in the simulation to present the mean values for the 5-gait cycle. A static optimization method was performed to predict the forces in 3D for the tibiofemoral force and 6 lower limb muscles. The 2nd Newton law in 3D was considered as the nonlinear constraints for the optimization process. The model considered the shank and

the foot as one element during the simulation to avoid more calculation of the internal force at the ankle, unlike traditional inverse kinematics.

For subject A, the 1st peak for medial and lateral tibiofemoral forces was 2.34 ± 0.1 BW and 1.37 ± 0.2 BW, respectively, whereas for the 2nd peak was about 1.65 ± 0.2 BW and 0.89 ± 0.4 BW, respectively. On the other hand, for subject B, the 1st peak for medial and lateral tibiofemoral forces was 1.6 ± 0.2 BW and 1.48 ± 0.3 BW, respectively, whereas the for 2nd peak was about 0.5 ± 0.4 BW and 0.6 ± 0.1 BW, respectively. RMSE for subject A was 0.3 and 0.16 BW and for the subject, B was 0.15 and 0.12 BW for the medial and lateral tibiofemoral force respectively. Although, subject B had more accuracy than subject A for tibiofemoral force prediction, the two subjects were within the range of the force prediction as shown in Table. 1 and these results agreed to the results in the literature for both experimental measurements [40], [41] and model prediction [10], [42]. Moreover, a subject of TKR with e-tibia from the 4th grand challenge competition was used to achieve the validity of the model by comparing the tibiofemoral force prediction with measured e-tibia where the RMSE was 0.14, 0.09 and 0.19 BW for the medial, lateral and total tibia compartments. The diversity between people makes a generic model for prediction of the tibiofemoral force is a difficult task and that is why many competitions were held by ASME for that [6], [15] and many authors worked hard to achieve the best model [7], [43].

The muscles' forces were based on the moment arm calculation and the prediction of the force using static optimization. The estimated moment arms were compared to three literature data Buford [18], Spoor [18], and Arnold [8] to show the fidelity and ability to use the model for other motor tasks like running. The coefficient of concordance was used for comparing the agreement between the EMG signals and the predicted muscles' force[34]. The active/inactive threshold was considered 5% of the maximum value for both quantities [44]. Four muscles were used for concordance analysis; vasti, rectus femoris, gastrocnemius and biceps femoris (other muscles were not measured). The results were within the range of the literature [45] for the prediction of muscle force. The muscles' pattern was tested by comparing the prediction muscles force to scaled EMG signals to be in the range of the muscles force prediction as shown in Fig.8

While Optimization could be used for the prediction of the tibiofemoral and muscle forces based on the sum square of the forces or the muscles activations with different constraints [46], the prediction of the forces was based on the constraints [47]. Our model was based on the force and moment of both the muscles and tibiofemoral force in 3D as the constraints with neglecting the patella and the ligaments force. The predicted muscles' forces were compared to the EMG signals pattern and the values as shown in Fig.8 and Table 3. The results showed that the model could predict some muscles with high accuracies like rectus femoris for both subjects(R^2) 0.83 and 0.64 for subjects A and B, respectively. In addition, the model introduced good agreement for vasti

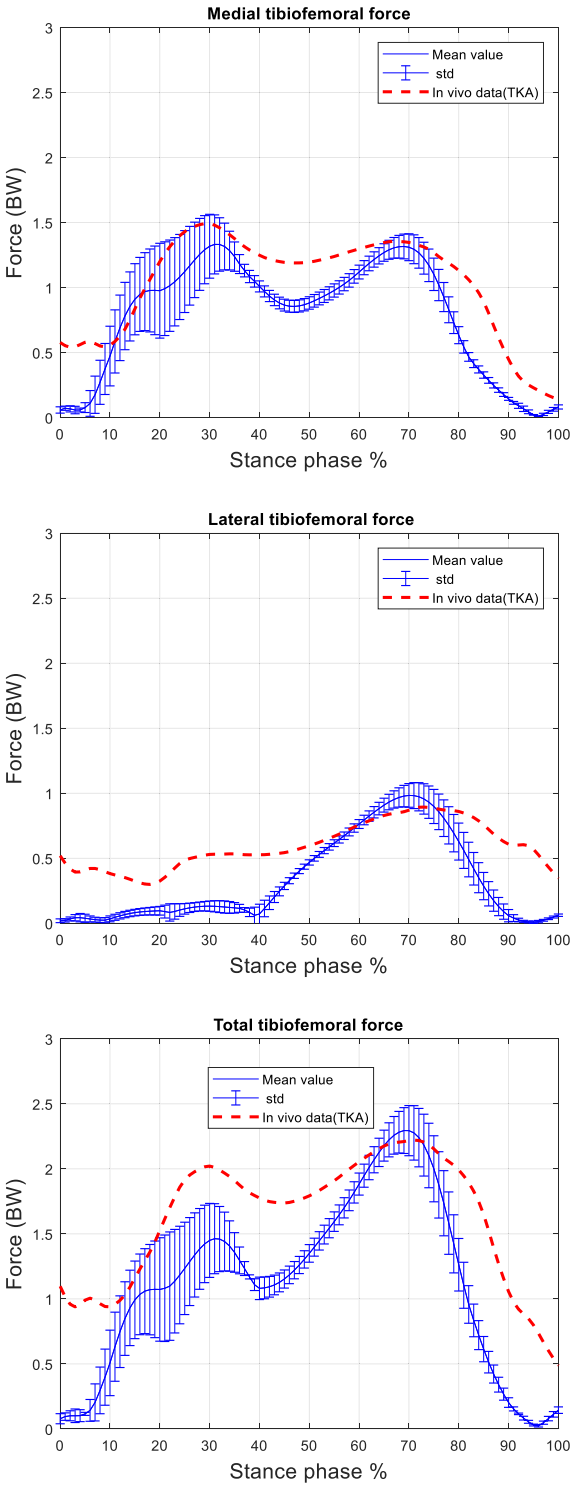

FIGURE 9. The tibiofemoral force for a subject of TKR. the tibiofemoral force prediction (solid blue line) and standard deviation (vertical bars) and the corresponding measured in vivo data (dotted red line [6].

(R^2 = 0.53) for subject A and gastrocnemius (R^2 = 0.55) and biceps femoris (R^2 = 0.67) for subject B. Moreover, the maximum values for all muscles force was within the range of predicted muscles in the literature [47], [48]. Moreover, the RMSE for rectus femoris, vasti and biceps femoris didn't

exceed 0.1 BW for both subjects and only the gastrocnemius had 0.18 and 0.28 BW for subject A and B respectively.

The values of the muscles force were different during the 5 gait cycles and that agreed with the EMG signals. The analysis of the maximum value of each muscle force by comparing it with the literature data showed the validity of the predicted muscles' force. The gastrocnemius had a maximum value of 0.75 BW for subject A and the literature showed 1.54 ± 0.7 BW[48] while subject B had 1.22 BW. Vasti had a maximum value of 0.42 and 0.34 BW for both subjects within the range of literature. Biceps femoris had a similar value for both subjects 0.16, 0.26 BW where Moissenet *et al.*, 2012 [47] prediction was 0.15 BW. For hamstring muscles, the maximum values were 0.12 and 0.25 BW where they were in the literature 0.67 ± 0.5 BW [48]. Rectus femoris maximum values were 0.18 and 0.14 BW for both subjects and other publication summarized as 0.4 ± 0.3 BW [48]. The tensor fasciae latae had a maximum value of 0.005 and 0.017 BW for both subjects and that may be expected due to the small PSCA compared to other muscles.

The study had some limitations to be overcome in future work. Firstly, the study was performed for only two healthy subjects. However, the model was validated with the ground truth of the subject had TKR from the 4th grand challenge competition [6]. Secondly, the EMG signals can't be measured for all the lower limb muscles since a few muscles can be measured in vivo. However different methods for the validation of predicted muscle force were used such as the coefficient of determination (R^2) and the coefficient of concordance for comparing the pattern of the predicted muscles forces with the available EMG signals, in addition to, comparing with the data in the literature. Thirdly, the patella force and the ligaments were not introduced in the model. However, the effect of the patella was considered during the estimation of the muscle's moment arm for the vast and rectus femoris using the helical axis to represent the motion of the patella w.r.t the knee. Also, the direction of these muscles' forces was reversed to simulate the effect of the patella tendon on the tibia during the motion. Finally, the cost function for optimization was based on weight factors and that may be different from one subject to another. However, the results of the prediction were with the literature results [7], [37]–[39], [49], in Table 1

VII. CONCLUSION

A model for the prediction of the muscle and tibiofemoral forces is proposed to avoid the high-cost computation of the traditional inverse dynamic method. The model has considered the shank and the foot as one element and so the forces and moments at the ankle are not estimated while the kinematics, weight, and inertia of each segment have been considered during the analysis. Additionally, the model does not include the EMG signals to predict the muscle and tibiofemoral forces to avoid the problem of time-consuming filtering and process the signals. The model has been performed on two healthy subjects walking at 1m/sec. The model has shown good accuracy in the prediction of the tibiofemoral forces by comparing it to in vivo e-tibia measurement of TKA subject. Also, the model has proved a reasonable prediction for the muscle's forces comparing to the scaled EMG signals. The model has guaranteed validity and accuracy by implementing on TKR subject as ground truth and two healthy subjects, where the results are within the range of literature data. The model is standalone where no need for other software to estimate the muscle moment arm, unlike OpenSim. The moment arms of the muscles were verified by comparing to the measured data and that guarantees using the model in other activities and applications that need high knee flexion angle like running. Using the 3DOF knee joint, introducing the knee ligament, lower limb muscles, and subject-specific tibiofemoral points of contact in the model are future objectives to enhance the model.

APPENDIX A

The direction of the tibiofemoral force is based on the vector P_{cf} of the contact point at each condyle. The differentiating of this vector w.r.t X and Z produces two vectors $\frac{\partial P_{cf}}{\partial x}$ and $\frac{\partial P_{cf}}{\partial z}$ in the X and Z direction, respectively. The cross product of these two vectors produces vectors;n_f and n_t normal to the surface of the femur and the tibia at the contact points, respectively. (1A).

$$\begin{aligned}
P_{cf} &= x\hat{i} + y\hat{j} + z\hat{k} \\
y &= f(x, z) \\
\frac{\partial P_{cf}}{\partial z} &= 0\hat{i} + \frac{\partial y}{\partial z}\hat{j} + \hat{k} \\
\frac{\partial \mathrm{P_{cf}}}{\partial x} &= \hat{i} + \frac{\partial y}{\partial x}\hat{j} + 0\hat{k} \\
n_f &= \frac{\partial P_{cf}}{\partial x} x \frac{\partial P_{cf}}{\partial z} \\
n_f &= \frac{\partial y}{\partial x}\hat{i} - \hat{j} + \frac{\partial y}{\partial z}\hat{k} \\
\hat{n}_f &= \frac{n_f}{\parallel n_f \parallel} = \frac{\frac{\partial y}{\partial x}\hat{i} - \hat{j} + \frac{\partial y}{\partial z}\hat{k}}{\sqrt{(\frac{\partial y}{\partial x})^2 + (\frac{\partial y}{\partial z})^2 + 1}}
\end{aligned} \tag{1A}$$

As the medial and lateral femur condyles are represented as part of spheres as shown in (1,2) in the paper, the normal vector on the femur condyles can be presented by (2A), and(3A).

$$\begin{aligned}
y &= -\sqrt{r_{fm}^2 - (x - a_1)^2 - (z - c_1)^2} + b_1 \\
\frac{\partial y}{\partial x} &= \frac{(x - a_1)}{\sqrt{r_{fm}^2 - (x - a_1)^2 - (z - c_1)^2}} \\
\frac{\partial y}{\partial z} &= \frac{(z - c_1)}{\sqrt{r_{fm}^2 - (x - a_1)^2 - (z - c_1)^2}} \\
\hat{n}_f &= \frac{n_f}{\parallel n_f \parallel} = \frac{\frac{\partial y}{\partial x}\Big|_{(x_c, z_c)}\hat{i} - \hat{j} + \frac{\partial y}{\partial z}\Big|_{(x_c, z_c)}\hat{k}}{\sqrt{\frac{r_{fm}^2}{r_{fm}^2 - (x - a_1)^2 - (z - c_1)^2}}}
\end{aligned} \tag{2A}$$

$$\hat{n}_f = \frac{n_f}{\| n_f \|} = \frac{\frac{\partial y}{\partial x}\Big|_{(x_c,z_c)} \hat{i} - \hat{j} + \frac{\partial y}{\partial z}\Big|_{(x_c,z_c)} \hat{k}}{\sqrt{\frac{r_{fm}^2}{r_{fm}^2-(x-a_1)^2-(z-c_1)^2}}} \tag{3A}$$

The two-unity vectors normal to the femur and the tibia are collinear at the points of contact and so $\hat{n}_t = \hat{n}_f$ where $\hat{n}_{t(medial)}$ and $\hat{n}_{t(lateral)}$ are the normal vectors at the medial and lateral tibia compartment, respectively.

$$\begin{bmatrix} F_x \\ F_y \\ F_z \end{bmatrix}_{medial} = F_{cont(medial)}.\hat{n}_{t\,(medial)} \tag{4A}$$

$$\begin{bmatrix} F_x \\ F_y \\ F_z \end{bmatrix}_{lateral} = F_{cont(lateral)}.\hat{n}_{t\,(lateral)} \tag{5A}$$

APPENDIX B

The constraints of the optimization process are based on the 2nd Newton law after modifying (1) and (2) to be (1B) and (2B), respectively. Nonlinear equality constraints are based on (1B) by checking the value of the forces affecting the knee at each knee angle to be within the constraints for predicting the muscles and the tibiofemoral forces. On the other hand, the linear equality constrains A_{equ}, and B_{equ} are based on (2B). The cost function of optimization should have a scalar value of the forces to be run and optimized. Additionally, it is required to tune the medial and lateral tibiofemoral forces in 3D. Using the direction of tibiofemoral forces $\hat{n}_f$ in 3D (2A) and (3A) and muscles potential moment vector (cross product between the vector from knee joint to the insertion point and the unit vector of muscle force line of action), the magnitude of the predicted forces can be separated from the direction (2B). Using the screw matrix to represent the cross product between the moment arm and unit vector of each force line of action (5.4), in that A_{equ} is a (3 × 24) matrix(3B). Also, B_{equ} equals (M_T); a (3 × 1) vector of the moment that affect the knee in 3D (2B).

$$\begin{bmatrix} F_{cont-x} \\ F_{cont-y} \\ F_{cont-z} \end{bmatrix} + \sum_{i=1}^{i=n} \begin{bmatrix} F_{\text{i}\,musc\,x} \\ F_{i\,musc\,y} \\ F_{\text{i}\,musc\,z} \end{bmatrix} = C$$

where

$$\text{C} = m \begin{bmatrix} \ddot{x} \\ \ddot{y} \\ \ddot{z} \end{bmatrix} + \begin{bmatrix} GRF_x \\ GRF_y \\ GRF_z \end{bmatrix} + \begin{bmatrix} w_x \\ w_y \\ w_z \end{bmatrix} \tag{1B}$$

$$r_{cont} \times \overleftarrow{F}_{cont} + r_{imuscles} \times \overleftarrow{F}_{\text{i muscles}} = \text{M}_T$$

$$\overleftarrow{F}_{cont} = \hat{n}_f \cdot F_{cont}$$

$$\overleftarrow{F}_{\text{i musc}} = pmv \cdot F_{\text{i musc}}$$

$$\begin{bmatrix} r_{cont} \times \hat{n}_f & r_{\text{i musc}} \times pmv \end{bmatrix} \begin{bmatrix} F_{\text{tibiofemoral}} \\ F_{\text{i muscles}} \end{bmatrix} = \text{M}_T$$

where

$$M_{inertia} = \begin{bmatrix} I_{xx}\ddot{\theta}_x \\ I_{yy}\ddot{\theta}_y \\ I_{zz}\ddot{\theta}_z \end{bmatrix} + \begin{bmatrix} (I_{zz} - I_{yy}) \\ (I_{xx} - I_{zz}) \\ (I_{yy} - I_{xx}) \end{bmatrix} \begin{bmatrix} \dot{\theta}_y\dot{\theta}_z \\ \dot{\theta}_x\dot{\theta}_z \\ \dot{\theta}_x\dot{\theta}_y \end{bmatrix}$$

$$\text{M}_T = M_{inertia} + r_{GRM} \times GRF + r_g \times \text{w}$$

$$A_{equ} = [r] \tag{2B}$$

where r represnts $r_{cont} \times \hat{n}_f or\ pmv$

$$A_{equ} = \begin{bmatrix} 0 & -A_{equ}\,(3) & A_{equ}\,(2) \\ A_{equ}\,(3) & 0 & -A_{equ}\,(1) \\ -A_{equ}\,(2) & A_{equ}\,(1) & 0 \end{bmatrix} \tag{3B}$$

REFERENCES

[1] S. D. Masouros, A. M. J. Bull, and A. A. Amis, "(i) biomechanics of the knee joint," *Orthopaedics Trauma*, vol. 24, no. 2, pp. 84–91, 2010.
[2] Y. Feng, T.-Y. Tsai, J.-S. Li, S. Wang, H. Hu, C. Zhang, H. E. Rubash, and G. Li, "Motion of the femoral condyles in flexion and extension during a continuous lunge," *J. Orthopaedic Res.*, vol. 33, no. 4, pp. 591–597, Apr. 2015.
[3] X. Zeng, L. Ma, Z. Lin, W. Huang, Z. Huang, Y. Zhang, and C. Mao, "Relationship between Kellgren-Lawrence score and 3D kinematic gait analysis of patients with medial knee osteoarthritis using a new gait system," *Sci. Rep.*, vol. 7, no. 1, pp. 1–8, Dec. 2017.
[4] S. K. Van De Velde, J. T. Bingham, T. J. Gill, and G. Li, "Analysis of tibiofemoral cartilage deformation in the posterior cruciate ligament-deficient knee," *J. Bone Joint Surg.-Amer. Volume*, vol. 91, no. 1, pp. 167–175, Jan. 2009.
[5] J. T. Bingham, R. Papannagari, S. K. Van De Velde, C. Gross, T. J. Gill, D. T. Felson, H. E. Rubash, and G. Li, "*In vivo* cartilage contact deformation in the healthy human tibiofemoral joint," *Rheumatology*, vol. 47, no. 11, pp. 1622–1627, Nov. 2008.
[6] B. J. Fregly, T. F. Besier, D. G. Lloyd, S. L. Delp, S. A. Banks, M. G. Pandy, and D. D. D'Lima, "Grand challenge competition to predict *in vivo* knee loads," *J. Orthopaedic Res.*, vol. 30, no. 4, pp. 503–513, Apr. 2012.
[7] R. Dumas, A. Zeighami, and R. Aissaoui, "Knee medial and lateral contact forces computed along subject-specific contact point trajectories of healthy volunteers and osteoarthritic patients," in *Computer Methods, Imaging and Visualization in Biomechanics and Biomedical Engineering*, 2020, pp. 457–463.
[8] E. M. Arnold, S. R. Ward, R. L. Lieber, and S. L. Delp, "A model of the lower limb for analysis of human movement," *Ann. Biomed. Eng.*, vol. 38, no. 2, pp. 269–279, Feb. 2010.
[9] M. D. K. Horsman, H. F. J. M. Koopman, F. C. T. van der Helm, L. P. Prosé, and H. E. J. Veeger, "Morphological muscle and joint parameters for musculoskeletal modelling of the lower extremity," *Clin. Biomech.*, vol. 22, no. 2, pp. 239–247, Feb. 2007.
[10] P. Gerus, M. Sartori, T. F. Besier, B. J. Fregly, S. L. Delp, S. A. Banks, M. G. Pandy, D. D. D'Lima, and D. G. Lloyd, "Subject-specific knee joint geometry improves predictions of medial tibiofemoral contact forces," *J. Biomech.*, vol. 46, no. 16, pp. 2778–2786, Nov. 2013.
[11] F. Moissenet, L. Modenese, and R. Dumas, "Alterations of musculoskeletal models for a more accurate estimation of lower limb joint contact forces during normal gait: A systematic review," *J. Biomech.*, vol. 63, pp. 8–20, Oct. 2017.
[12] H. J. Lundberg, K. C. Foucher, T. P. Andriacchi, and M. A. Wimmer, "Direct comparison of measured and calculated total knee replacement force envelopes during walking in the presence of normal and abnormal gait patterns," *J. Biomech.*, vol. 45, no. 6, pp. 990–996, Apr. 2012.
[13] M. A. Marra, M. S. Andersen, M. Damsgaard, B. F. J. M. Koopman, D. Janssen, and N. Verdonschot, "Evaluation of a surrogate contact model in force-dependent kinematic simulations of total knee replacement," *J. Biomech. Eng.*, vol. 139, no. 8, pp. 1–10, Aug. 2017.
[14] Z. Ding, D. Nolte, C. Kit Tsang, D. J. Cleather, A. E. Kedgley, and A. M. J. Bull, "*In vivo* knee contact force prediction using patient-specific musculoskeletal geometry in a segment-based computational model," *J. Biomech. Eng.*, vol. 138, no. 2, pp. 1–9, Feb. 2016
[15] A. L. Kinney, T. F. Besier, D. D. D'Lima, and B. J. Fregly, "Update on grand challenge competition to predict *in vivo* knee loads," *J. Biomech. Eng.*, vol. 135, no. 2, pp. 1–4, Feb. 2013.
[16] T. Finni, P. V. Komi, and J. Lukkariniemi, "Achilles tendon loading during walking: Application of a novel optic fiber technique," *Eur. J. Appl. Physiol.*, vol. 77, no. 3, pp. 289–291, Feb. 1998.
[17] I. B. Prilutsky and V. M. Zatsiorsky, "Optimization-based models of muscle coordination," *Bone*, vol. 23, no. 1, pp. 1–7, 2011.

[18] W. L. Buford, F. M. Ivey, J. D. Malone, R. M. Patterson, G. L. Pearce, D. K. Nguyen, and A. A. Stewart, "Muscle balance at the knee-moment arms for the normal knee and the ACL-minus knee," *IEEE Trans. Rehabil. Eng.*, vol. 5, no. 4, pp. 367–379, Dec. 1997.
[19] C. W. Spoor and J. L. van Leeuwen, "Knee muscle moment arms from MRI and from tendon travel," *J. Biomech.*, vol. 25, pp. 201–206, Feb. 2016.
[20] S. Pal, J. E. Langenderfer, J. Q. Stowe, P. J. Laz, A. J. Petrella, and P. J. Rullkoetter, "Probabilistic modeling of knee muscle moment arms: Effects of methods, Origin–insertion, and kinematic variability," *Ann. Biomed. Eng.*, vol. 35, no. 9, pp. 1632–1642, Aug. 2007.
[21] A. Erdemir, S. McLean, W. Herzog, and A. J. van den Bogert, "Model-based estimation of muscle forces exerted during movements," *Clin. Biomech.*, vol. 22, no. 2, pp. 131–154, Feb. 2007.
[22] B. A. Knarr and J. S. Higginson, "Practical approach to subject-specific estimation of knee joint contact force," *J. Biomech.*, vol. 48, no. 11, pp. 2897–2902, Aug. 2015.
[23] K. Sasaki, R. R. Neptune, and S. A. Kautz, "The relationships between muscle, external, internal and joint mechanical work during normal walking," *J. Experim. Biol.*, vol. 212, no. 5, pp. 738–744, Mar. 2009.
[24] N. Sancisi, X. Gasparutto, V. Parenti-Castelli, and R. Dumas, "A multibody optimization framework with a knee kinematic model including articular contacts and ligaments," *Meccanica*, vol. 52, no. 3, pp. 695–711, Feb. 2017.
[25] R. Dumas, L. Cheze, and F. Moissenet, "Multibody optimisations: From kinematic constraints to knee contact forces and ligament forces," in *Springer Tracts in Advanced Robotics*, vol. 124. Cham, Switzerland: Springer, 2019, pp. 65–89.
[26] J. Wojtusch and O. Von Stryk, "HuMoD—A versatile and open database for the investigation, modeling and simulation of human motion dynamics on actuation level," in *Proc. IEEE-RAS Int. Conf. Humanoid Robots*, Nov. 2015, pp. 74–79.
[27] A. D. Kuo, "A least squares estimation approach to improving the precision of inverse dynamics computations," *J. Biomech. Eng.*, vol. 120, no. 1, pp. 148–159, 1995.
[28] A. L. Hof, "An explicit expression for the moment in multibody systems," *J. Biomech.*, vol. 25, no. 10, pp. 1209–1211, Oct. 1992.
[29] G. Wu and P. R. Cavanagh, "ISB recommendations for standardization in the reporting of kinematic data," *J. Biomech.*, vol. 28, no. 10, pp. 1257–1261, Oct. 1995.
[30] R. Nisell, G. Németh, and H. Ohlsén, "Joint forces in extension of the knee: Analysis of a mechanical model," *Acta Orthopaedica Scandinavica*, vol. 57, no. 1, pp. 41–46, Jan. 1986.
[31] E. M. Abdel-Rahman and M. S. Hefzy, "Three-dimensional dynamic behaviour of the human knee joint under impact loading," *Med. Eng. Phys.*, vol. 20, no. 4, pp. 276–290, Jun. 1998.
[32] P. Sritharan, Y.-C. Lin, and M. G. Pandy, "Muscles that do not cross the knee contribute to the knee adduction moment and tibiofemoral compartment loading during gait," *J. Orthopaedic Res.*, vol. 30, no. 10, pp. 1586–1595, Oct. 2012.
[33] R. J. Butler, S. Marchesi, T. Royer, and I. S. Davis, "*In vivo* medial and lateral tibial loads during dynamic and high flexion activities," *J. Orthopaedic Res. September*, vol. 25, no. 5, pp. 1121–1127, 2007.
[34] M. Giroux, F. Moissenet, and R. Dumas, "EMG-based validation of musculo-skeletal models for gait analysis," *Comput. Methods Biomechanics Biomed. Eng.*, vol. 16, no. 1, pp. 152–154, Jul. 2013.
[35] S. L. Delp, J. P. Loan, M. G. Hoy, F. E. Zajac, E. L. Topp, and J. M. Rosen, "An interactive graphics-based model of the lower extremity to study orthopaedic surgical procedures," *IEEE Trans. Biomed. Eng.*, vol. 37, no. 8, pp. 757–767, 1990.
[36] R. M. Ehrig, W. R. Taylor, G. N. Duda, and M. O. Heller, "A survey of formal methods for determining the centre of rotation of ball joints," *J. Biomech.*, vol. 39, no. 15, pp. 2798–2809, Jan. 2006.
[37] F. Moissenet, L. Chèze, and R. Dumas, "Influence of the level of muscular redundancy on the validity of a musculoskeletal model," *J. Biomech. Eng.*, vol. 138, no. 2, pp. 1–23, Feb. 2016.
[38] S. Meireles, M. Wesseling, C. R. Smith, D. G. Thelen, S. Verschueren, and I. Jonkers, "Medial knee loading is altered in subjects with early osteoarthritis during gait but not during step-up-and-over task," *PLoS ONE*, vol. 12, no. 11, pp. 1–20, 2017.
[39] S. Van Rossom, N. Khatib, C. Holt, D. Van Assche, and I. Jonkers, "Subjects with medial and lateral tibiofemoral articular cartilage defects do not alter compartmental loading during walking," *Clin. Biomech.*, vol. 60, pp. 149–156, Dec. 2018.
[40] I. Kutzner, B. Heinlein, F. Graichen, A. Bender, A. Rohlmann, A. Halder, A. Beier, and G. Bergmann, "Loading of the knee joint during activities of daily living measured *in vivo* in five subjects," *J. Biomech.*, vol. 43, no. 11, pp. 2164–2173, Aug. 2010.
[41] D. D. D'Lima, S. Patil, N. Steklov, S. Chien, and C. W. Colwell, "*In vivo* knee moments and shear after total knee arthroplasty," *J. Biomech.*, vol. 40, pp. S11–S17, Jan. 2007.
[42] H. J. Lundberg, C. Knowlton, and M. A. Wimmer, "Fine tuning total knee replacement contact force prediction algorithms using blinded model validation," *J. Biomech. Eng.*, vol. 135, no. 2, pp. 1–9, Feb. 2013.
[43] M. Cardona and C. E. G. Cena, "Biomechanical analysis of the lower limb: A full-body musculoskeletal model for muscle-driven simulation," *IEEE Access*, vol. 7, pp. 92709–92723, 2019.
[44] H. Suzuki, R. A. Conwit, D. Stashuk, L. Santarsiero, and E. J. Metter, "Relationships between surface-detected EMG signals and motor unit activation," *Med. Sci. Sports Exerc.*, vol. 34, no. 9, pp. 1509–1517, Sep. 2002.
[45] F. Moissenet, L. Chèze, and R. Dumas, "A 3D lower limb musculoskeletal model for simultaneous estimation of musculo-tendon, joint contact, ligament and bone forces during gait," *J. Biomech.*, vol. 47, no. 1, pp. 50–58, Jan. 2014.
[46] Y.-C. Lin, J. P. Walter, S. A. Banks, M. G. Pandy, and B. J. Fregly, "Simultaneous prediction of muscle and contact forces in the knee during gait," *J. Biomechanics*, vol. 43, no. 5, pp. 945–952, Mar. 2010.
[47] F. Moissenet, L. Chèze, and R. Dumas, "Anatomical kinematic constraints: Consequences on musculo-tendon forces and joint reactions," *Multibody Syst. Dyn.*, vol. 28, nos. 1–2, pp. 125–141, Aug. 2012.
[48] U. K. Trinler, "Muscle force estimation in clinical gait analysis muscle force estimation in clinical gait analysis," Univ. Salford, Salford, U.K., 2016. [Online]. Available: http://usir.salford.ac.uk/id/eprint/39257
[49] S. Meireles, F. De Groote, S. Van Rossom, S. Verschueren, and I. Jonkers, "Differences in knee adduction moment between healthy subjects and patients with osteoarthritis depend on the knee axis definition," *Gait Posture*, vol. 53, pp. 104–109, Mar. 2017.

ALI MAMDOUH MOHAMED received the B.E. degree in Mechanical Power Engineering from the Faculty of Engineering, Tanta University, Egypt, in 2009, the Diploma degree in mechatronics from the Information Technology Institute (ITI), Egypt, in 2010, and the master's degree in mechatronic and robotics from the Faculty of Engineering, Tanta University, in 2015. He is currently pursuing the Ph.D. degree with the School of Mechanical Science and Engineering, Huazhong University of Science and Technology (HUST), China. He is currently an Assistant Lecturer with the Mechanical Power Engineering Department, Faculty of Engineering, Tanta University. His research interests include robotics, biomechanics, automation, and control.

RONGLEI SUN received the B.E. degree in industrial automation and the Ph.D. degree in mechatronic engineering from the Huazhong University of Science and Technology (HUST), China, in 1985 and 2002, respectively. He is currently a Professor with the School of Mechanical Science and Engineering, HUST. His research interests include robotics, biomechanics, machine learning, and computer vision.